IEEE Open Journal of
Vehicular Technology

Received 19 December 2025; accepted 7 January 2026. Date of publication 12 January 2026;
date of current version 2 February 2026. The review of this article was coordinated by Editor Lipeng Zhu.

Digital Object Identifier 10.1109/OJVT.2026.3652908

Resource Allocation Schemes for Scalable Panel-Based LIS Surfaces

ANDREIA PEREIRA [1,2], FILIPE CONCEIÇÃO [1,2] (Graduate Student Member, IEEE), FREDRIK RUSEK [3], RUI DINIS [1,4] (Senior Member, IEEE), AND MARCO GOMES [1,2] (Senior Member, IEEE)

[1]Instituto de Telecomunicações, 3030-290 Coimbra, Portugal
[2]Department of Electrical and Computer Engineering, University of Coimbra, 3030-290 Coimbra, Portugal
[3]Sony Europe B.V., 221 88 Lund, Sweden
[4]FCT-UNL, 2829-516 Caparica, Portugal

CORRESPONDING AUTHOR: FILIPE CONCEIÇÃO (e-mail: filipe.conceicao@co.it.pt).

The work of Andreia Pereira, Filipe Conceição, Rui Dinis, and Marco Gomes was supported by the National Funds through FCT Fundação para a Ciência e a Tecnologia, I.P., and, when eligible, co-funded by EU funds under Project/Support UID/50008/2025 – Instituto de Telecomunicações, with DOI identifier https://doi.org/10.54499/UID/50008/2025, PhD Grant SFRH/BD/137745/2018, and the Research Grant LA/P/0109/2020. The work of Fredrik Rusek was supported by Swedish Research Council (VR).

ABSTRACT Panel-based large intelligent surface (LIS) systems, where each panel comprises a lower, but significant, number of antennas, and is equipped with several baseband outputs (generally much smaller than the number of terminals), allow for a direct dimensionality reduction. However, such dimensionality reduction may not be enough to simplify the overall system. This paper focuses on fully decentralized system architectures that allow for promising performances while requiring low, or even no, central data processing. This paper proposes panel-selection and panel-terminal association algorithms for decentralized panel-based LIS communication systems aiming at allocating a set of terminals to a given panel, which is limited to a given number of outputs, in a sequential or flooding manner, while maximising the minimum terminal rate. Performance results show that sequential and flooding distributed system architectures offer decent convergence rates in comparison with a centralized system architectures when selecting a proper combination of system parameters (number of panels, number of terminals, number of baseband outputs), in turn ensuring scalability. It is shown that, for a given combination of the system parameters, a max-min terminal rate achieved when considering sequential and flooding distributed system architectures can converge to the one achieved by the centralized system architecture, occurring after just a few iterations. Both the proposed sequential and flooding algorithms represent a less complex, but effective way to perform both panel selection and panel-terminal association, allowing for the deactivation of a significant portion of panels without substantially degrading the max-min terminal rate achieved by the centralized system architecture.

INDEX TERMS Large Intelligent surfaces, massive MIMO, spatial resource allocation, sequential optimisation, flooding optimisation, massive MIMO.

I. INTRODUCTION

Panel-based large intelligent surface (LIS) systems, where each panel comprises a lower, but still significant, number of antennas, and is equipped with a number of baseband outputs (generally much smaller than the number of terminals), allows for a direct dimensionality reduction.

Panel-based LIS systems envision hierarchical processing [1], with each panel (e.g., construed as local processing unit (LPU) or an LPU in communication with each panel) providing its respective output to a central processing unit (CPU) that combines it with outputs from other panels. However, as the number of antennas grows, implementation of centralized system architectures (e.g., addressed in [2], [3]) may become more challenging and such a dimensionality reduction may not be enough to simplify the overall system. As an example, the inter-connection bandwidths to/from the CPU may be limiting factor.

Hence, it may be desirable to have less amount of data to be collected by an CPU for baseband processing. Therefore, it is crucial to design algorithms for fully decentralized system

© 2026 The Authors. This work is licensed under a Creative Commons Attribution 4.0 License. For more information, see https://creativecommons.org/licenses/by/4.0/

architectures that allow for promising performances while requiring low, or even no, central data processing.

Decentralized system architectures have been explored in the context of massive multiple-input multiple-output (m-MIMO) [4], [5], [6], [7], LIS [8], [9], [10], [11], cell-free [12], [13], [14], [15], [16], [17] and radio stripes [18], [19], [20], [21], [22] based systems, focusing on the development of uplink detection algorithms based on zero forcing (ZF) as well as variants of maximum ratio combining (MRC) (or matched filtering (MF)) for interference suppression purposes. In particular, [8] proposes a fully decentralized algorithm for constructing an approximate ZF equalizer for an LIS. Authors in [8] introduce an iterative message-passing algorithm that involves repeated exchanges of a specific measure between each antenna of a grid of antennas and its neighbouring antennas, with the message routing carefully designed to avoid redundancy. Specifically, as this measure propagates across the entire grid of antennas, it gradually loses influence on interference cancellation updates at distant antennas because newer updates and contributions take precedence.

A joint panel-selection and panel-terminal association for a centralized system architecture is proposed in [2], [3], where the corresponding optimisation problem is a mixed-integer linear programming (MILP) solved using an MILP solver. In addition, authors in [23] propose a sequential system architecture for panel selection and panel-terminal association optimization purposes, which requires no central data processing, in order to overcome the implementation challenges inherent to centralized system architectures.

This paper investigates the conditions under which the performance achieved by a sequential and flooding system architecture employing a panel selection and panel-terminal association algorithm becomes comparable to a centralized system architecture (e.g., proposed in [2], [3], while also proposing effective application strategies for both decentralized system architectures when employing such panel selection and panel-terminal association algorithm. The decentralized system architectures include the sequential system architecture proposed in [23] and a flooding system architecture using the iterative message-passing algorithm proposed in [8]. As previously discussed, the iterative message-passing algorithm has been proposed in [8] in the context of equalisation, being thus adapted for panel selection and panel-terminal association optimization purposes in this paper. The sequential system architecture has been proposed in [23] for panel selection and panel-terminal association optimization purposes, being in this paper compared to the adapted flooding system architecture. The joint panel selection and panel-terminal association algorithm aims at allocating a set of terminals to a given panel, the panel being limited to a number of baseband outputs, in a sequential [23] or flooding [8] manner, while maximising the minimum terminal rate. For the sequential system architecture, the panels can cooperate sequentially by passing around SINR information, containing a linear combination of all the SINR values for the set of terminals sent by all the previously processed panels. For the flooding system architecture, the panels which are arranged in a grid can cooperate by passing around SINR information containing a linear combination of the SINR values (which do not necessarily contain SINR information from all the panels, being therefore dependent on how many panels have already shared such information) for the set of terminals sent by the respective neighbouring panels.

In this paper, system parameters including the number of panels (P), the number of terminals to be served by a set of such panels (K), and the number of baseband outputs per panel (N) have been analysed for scalability purposes. The contributions of the present paper are described as follows:

- The iterative message-passing algorithm proposed by [8] has been adapted for panel selection and panel-terminal association optimization purposes. In particular, each active panel communicates an average aggregated SINR with one another according to the iterative message-passing algorithm properly adapted for panel selection and panel-terminal association optimization purposes. The iterative message-passing algorithm is adapted for such purposes by performing the joint panel selection and panel-terminal association in such a way that the minimum SINR among all terminals is maximized. In addition, the SINR information shared with a given panel includes KP SINR contributions from each of its neighbouring panels (either deactivated, and thus used as a bridge to transmit those SINR values from an active panel in communication with those deactivated panels, or active) averaged over a number of iterations, P denoting the number of panels and K denoting the number of terminals to be served by a subset of such panels;
- Provision of specific combinations of system parameters (including the number of panels, the number of terminals to be served by a set of such panels, and the number of baseband outputs per panel) required by the decentralized system architectures (i.e., sequential and flooding system architectures) to ensure full or approximate convergence to a max-min terminal rate achieved by the centralized system architecture;
- Provision of performance losses in the max-min terminal rate for a combination of system parameters yielding a proper convergence when considering either the sequential system architecture or the flooding system architecture relative to the centralized system architecture; and
- Comparison of the sequential system architecture and the flooding system architecture in terms of convergence to the max-min terminal rate of the centralized system architecture, number of outputs per panel for delivering a proper max-min terminal rate, and performance loss relative to the centralized system architecture.

A. NOTATION

Throughout this paper the following notation will be adopted: the operators $(\cdot)^*$ and $(\cdot)^H$ stand for the complex conjugate and the Hermitian transpose, respectively. Boldface letters (e.g. **a**) denote vectors and boldface uppercase letters (e.g. **A**) denote matrices. In particular, $a_{m,n}$ indicates the element at the mth row and nth column of matrix $\mathbf{A}$, a_m indicates the mth element of vector **a**.

II. SYSTEM CHARACTERISATION

An uplink transmission between K single antenna terminals and a panel-based LIS, comprising P panels arranged according to a squared (or rectangular) lattice, each one with M antennas and $N \ll M$ baseband outputs (as known as RF chains). It is also assumed that $N \ll K$, while $NP > K$, and therefore some resource allocation strategy is needed. It should be noted that a centralized system architecture considers an CPU for data aggregation (e.g., SINR measures) and resource allocation related decisions. A fully decentralized LIS-based system may contain a local processing unit (LPU) per panel (as opposed to a CPU), with each LPU being used for computation of a local SINR and resource allocation-related decisions. Computation of a local SINR and resource allocation-related decisions by LPUs can increase processing capacity without overloading an CPU, thus mitigating the complexity associated with a centralized architecture. In addition, as inter-connection bandwidths to/from the CPU may be a limiting factor in centralized system architectures, decentralized architectures may ensure that only relevant data is sent to the CPU, thereby reducing network congestion, and fronthaul signal overhead. In this paper, it is envisioned that the information communicated between panels is never sent to the CPU.

Assuming a narrowband communication system with each terminal radiating isotropically, the received signal at the pth LIS panel is given by,

$$\mathbf{y}_p = \left[y_p^{(1)}, \ldots, y_p^{(M)}\right]^T = \mathbf{G}_p \mathbf{J} \mathbf{x} + \mathbf{n}_p \ , \quad (1)$$

with $\mathbf{x} = [x_1, \ldots, x_K]^T$ and $\mathbf{n}_p = [n_p^{(1)}, \ldots, n_p^{(M)}]^T$, where x_k is the signal sent by the k-th terminal, and $y_p^{(m)}$ and $n_p^{(m)}$ are the signal and noise captured at the p-th panel's m-th antenna, respectively. $\mathbf{G}_p = [G_{p,(m,k)}]_{M\times K}$ is the channel matrix, with $G_{p,(m,k)}$ denoting the channel between the k-th terminal and the m-th antenna of the pth panel, and $\mathbf{J} = \mathrm{diag}\{\rho_1, \ldots, \rho_K\}$, where ρ_k is the transmit power of the kth terminal. $\mathbf{G}_p$ is characterised by multipath fading, pathloss and shadowing components as in [24], and is given by,

$$\mathbf{G}_p = \mathbf{H}_p \mathbf{D}_p^{1/2} \ , \quad (2)$$

where $\mathbf{H}_p = [H_{p,(m,k)}]_{M\times K}$ models the multipath fading, following an independent and identically distributed (i.i.d) Rayleigh fading model, whose coefficient $H_{p,(m,k)}$ follows a complex Gaussian distribution, i.e. $H_{p,(m,k)} \sim \mathcal{CN}(0,1)$. $\mathbf{D}_p = \mathrm{diag}\{d_{p,(1)}, \ldots, d_{p,(K)}\}$ represents the large-scale propagation component (i.e., the pathloss and shadowing) and,

$$d_{p,(k)} = \frac{z_{p,(k)}}{r_{p,(k)}^{\ell}} \ , \quad (3)$$

where $r_{p,(k)}$ denotes the Euclidean distance between the kth terminal and the centre of the pth panel, ℓ is the path loss exponent, and $z_{p,(k)}$ refers to the shadowing effect which follows a log-normal distribution, i.e., $10\log_{10}(z_{p,(k)}) \sim \mathcal{N}(0, \sigma_{\text{shad}})$. Independent shadow fading is also assumed over the different LIS panels.

In this paper, it is considered that for the panel-based LIS, each panel has perfect knowledge of its own channel matrix $\mathbf{G}_p$ (only), and such knowledge is used for detection and resource allocation, either using a centralized or a distributed system architecture.

III. UPLINK DETECTION AND SINR CALCULATION

The post-processed signal at the pth panel can be represented as,

$$\tilde{\mathbf{x}}_p = \mathbf{F}_p \mathbf{y}_p = \mathbf{F}_p \mathbf{G}_p \mathbf{J} \mathbf{x} + \mathbf{F}_p \mathbf{n}_p \ , \quad (4)$$

where $\mathbf{F}_p = [F_{p,(k,m)}]_{K\times M}$ denotes the equalisation matrix, $F_{p,(k,m)}$ is the equalisation coefficient of the k-th terminal and the m-th antenna of the p-th LIS panel, and $\mathbf{n}_p$ is assumed to be a zero-mean with a Gaussian distribution whose variance is related to a power spectral density of the noise N_0.

The MF equalisation technique is performed at each panel, where the received signals are phase corrected and weighted by the conjugate of the channel matrix. The MF receiver matrix for the pth panel can be given by,

$$\mathbf{F}_p = \mathbf{G}_p^H \ . \quad (5)$$

Combining (4) and (5) results in,

$$\tilde{\mathbf{x}}_p = [\tilde{x}_{p,(1)}, \ldots, \tilde{x}_{p,(K)}] = \mathbf{G}_p^H \mathbf{y}_p = \mathbf{R}_p \mathbf{x} + \mathbf{w}_p \ , \quad (6)$$

where $\tilde{x}_{p,(k)}$ denotes the estimation of the signal sent by the kth terminal at panel p (i.e., a post-processed signal) when employing the MF equalisation technique. $\mathbf{R}_p = \mathbf{G}_p^H \mathbf{G}_p$ denotes the channel Gram matrix, and $\mathbf{w}_p$ is assumed to be zero-mean with a complex Gaussian distribution with covariance $\mathbb{E}[\mathbf{w}_p \mathbf{w}_p^{\mathrm{H}}] = \mathbf{R}_p N_0$.

Because each panel has $N \ll K$ baseband outputs, decision upon terminals to served by the pth panel needs to take in account the set of SINRs at the pth panel with respect to each terminal, i.e., $\boldsymbol{\gamma}_p = [\gamma_{p,(1)}, \ldots, \gamma_{p,(K)}]$. Using (6), the SINR $\gamma_{p,(k)}$ of the kth terminal observed by the pth panel, is given by,

$$\gamma_{p,(k)} = \frac{\rho_k |R_{p,(k,k)}|^2}{\sum_{\ell=1,\ell\neq k}^{K} \rho_\ell |R_{p,(k,\ell)}|^2 + R_{p,(k,k)} N_0}, \quad (7)$$

where the numerator is the received power of the desired signal from the kth terminal, and the left and right terms of the denominator stand, respectively, for the interference caused by the other terminals, and the noise captured at the pth panel.

The following section addresses panel selection and panel-terminal association schemes considering centralized or distributed system architectures, using the SINR $\boldsymbol{\gamma}_p$ as a basis. It should be emphasized that the panel selection and panel-terminal association for centralized system architectures is addressed in [2], [3].

IV. PANEL SELECTION AND PANEL-TERMINAL ASSOCIATION FOR CENTRALIZED SYSTEM ARCHITECTURE

In this section, the panel selection and panel-terminal association in a centralized manner is addressed for a panel-based LIS system. A centralized system architecture assumes that P panels, each one with N baseband outputs, are connected to a CPU for data aggregation. When considering a joint panel selection and panel-terminal association, the CPU must choose a suitable set of panels and which terminals must be allocated to them. Hence, each panel needs to calculate, according to (7), its K possible SINR values $\gamma_{p,(k)}$ and report them. The CPU then processes all the KP reported SINR values, taking a decision on which $P_{\mathrm{a}} \leq P$ panels to activate, and which terminals to allocate to each one of those P_{a} panels. P_{a} denotes the number of panels to activate out of the P panels in order to determine the panel-terminal pairs according to the panel selection and panel terminal association algorithm (i.e., a fairness resource allocation algorithm). Therefore, the CPU's feedback to the pth panel is a tuple $(\tilde{z}_p, \mathbf{c}_p)$ where:

- $\tilde{z}_p \in \{1, 0\}$ indicates the activation or non-activation of the pth panel;
- $\mathbf{c}_p = [c_{p,(1)}, \ldots, c_{p,(K)}]$ is a binary vector, where $c_{k,p} \in \{1, 0\}$ indicates whether the kth terminal is served by the pth panel, and $\sum_{k=1}^{K} c_{p,(k)} = \tilde{z}_p N$ meaning that only N terminals can be served if the pth panel is activated.

To address the joint panel selection and panel-terminal association for the centralized system architecture, the CPU computes an aggregate SINR $\boldsymbol{\gamma}_{\mathrm{agg}} = [\gamma_{(1)}, \ldots, \gamma_{(K)}]$ for the set of K terminals, whose element $\gamma_{(k)}$ is given by,

$$\gamma_{(k)} = \sum_{p=1}^{P} c_{p,(k)} \gamma_{p,(k)} = \sum_{p=1}^{P} \tilde{\gamma}_{p,(k)} \; . \tag{8}$$

where $\tilde{\gamma}_{p,(k)} = c_{p,(k)} \gamma_{p,(k)}$.

In essence, having P_{a} active panels, with N baseband outputs per panel, the outputs allocated to the same terminal are linearly combined providing an aggregate SINR for that terminal. It is an ambition of this chapter to execute it in such a way that the minimum SINR $\gamma_{\min}$ among all terminals is maximised, and therefore, the CPU must solve an optimisation problem that can be formulated as,

$$\begin{aligned} \max_{c_{p,(k)},\, \tilde{z}_p} \quad & \gamma_{\min} \\ \text{subject to:} \quad & \sum_{p=1}^{P} c_{p,(k)} \gamma_{p,(k)} \geq \gamma_{\min}, \quad \forall k \in \{1, \ldots, K\}, \\ & \sum_{k=1}^{K} c_{p,(k)} = \tilde{z}_p N, \quad \forall p \in \{1, \ldots, P\}, \\ & \sum_{p=1}^{P} \tilde{z}_p = P_{\mathrm{a}}, \\ & c_{p,(k)},\ \tilde{z}_p \in \{0, 1\ \gamma_{\min} \in [0, +\infty). \end{aligned} \tag{9}$$

Note that the first constraint ensures that all terminals are served by at least one panel-output; the second one ensures that N terminals are served by every active panel; and the third constraint accounts for the number of panels to be activated within the panel-based LIS. Furthermore, a constraint is also included to ensure that all terminals are served by at least one panel-output, $NP_{\mathrm{a}} \geq K$. The max-min terminal rate achieved at the end of the optimisation process is,

$$R_{\min} = \mathbb{E}[\log_2(1+t)] = \mathbb{E}[\log_2(1+\min(\boldsymbol{\gamma}_{\mathrm{agg}}))] \; . \tag{10}$$

When considering only terminal-panel association for a fixed panel selection scheme, the formulation of problem (9) remains correct as long as $NP_{\mathrm{a}} \geq K$, only differing in the fact that the third restriction disappears (i.e., $\tilde{z}_p$ are now fixed), and the sum in the first restriction is carried along the P_{a} panels selected a priori.

Problem (9) is an MILP with $P(K+1)$ binary variables, and can be solved using an MILP solver, available for example in IBM ILOG CPLEX Optimiser (CPLEX). We intend to investigate means of obtaining comparable max-min terminal rates to that of the MILP solver, but performed in a more scalable manner in the sense that there is no CPU to collect the SINR measures coming from the different panels. The panel selection and panel-terminal association stages for a fully decentralized architecture are discussed in the next section.

V. PANEL SELECTION AND PANEL-TERMINAL ASSOCIATION FOR DISTRIBUTED SYSTEM ARCHITECTURE

In this section, we address panel selection and panel-terminal association in a distributed manner for a panel-based LIS system. This process can involve optimizing both stages jointly or individually, and can be implemented in a sequential or flooding manner.

A distributed panel-based LIS system assumes that P panels, each one containing N baseband outputs, do not have any CPU for data aggregation and resource allocation related decisions. In this case, each panel has an LPU with reasonable processing capabilities for the computation of a local SINR and resource allocation-related decisions, the processed data is shared with the other panels.

A. SEQUENTIAL SYSTEM ARCHITECTURE

A sequential system architecture assumes P panels to be sequentially connected according to a panel grid[1] as shown in Fig. 1. In addition, the panel P is in communication with panel having index 1 (i.e., the output of panel P is fed to the panel with index 1).

Panel selection and panel-terminal association are iterative processes. Within iteration i (with $i = 1, \ldots, I$), panel-terminal association is performed using a sequential SINR sharing scheme, with each panel being processed at a time, and locally performing terminal assignment. Such panel uses

[1]The sequential panel selection and panel-terminal association algorithm can be employed in any shaped panel-based LIS, as long as the information is shared sequentially.

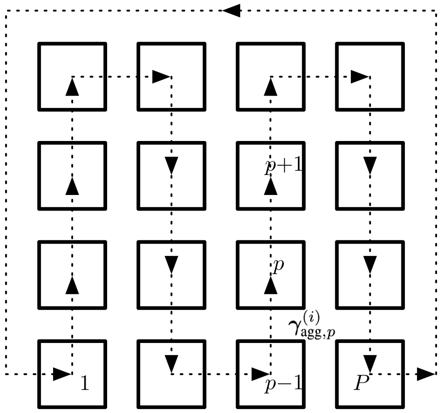

FIGURE 1. **Aggregate SINR spreading process over *P* panels when considering a sequential scheme, for a given round of communication. Each round of communication takes *P* steps, with the possibility of having it repeated over time, until an acceptable (or even optimum) max-min terminal rate is achieved.**

this information whether to remain active or to switch off. Regardless of the decision, an aggregate SINR incorporating such information is sent for the following panel.

Let $\boldsymbol{\gamma}^{(i)}_{\text{agg},p} = [\gamma^{(i)}_{\text{agg},p,(1)}, \ldots, \gamma^{(i)}_{\text{agg},p,(K)}]$ denote the set of aggregate SINRs for the K terminals, computed at the ith iteration by the pth panel. In particular, and as illustrated in Fig. 1, a given panel (e.g., the pth panel) receives an aggregate SINR $\boldsymbol{\gamma}^{(i)}_{\text{agg},p-1}$ from a previous panel. Such information is then used to perform local terminal assignment, in which a panel only selects N from the set of K terminals to serve, aiming at maximising the minimum SINR among all K terminals. Furthermore, if a panel chooses to remain active, based on the local terminal assignment, the aggregated SINR $\boldsymbol{\gamma}^{(i)}_{\text{agg},p}$ at the panel is updated and passed to the next one. In case a panel decides to switch off, it needs to simply pass the aggregated SINR coming from panel $p-1$ to panel $p+1$. In such an algorithm, no panel is turned off at iteration $i=1$. Instead, only panel-terminal association is performed to establish an initial max-min terminal rate achieved at panel P. Panel selection together with panel-terminal association are then performed for iterations $i>1$, taking into account the initial max-min terminal rate[2] provided by panel P at iteration i.

In order for the pth panel to choose which N terminals to serve that maximise the minimum SINR among all of them, a new optimisation problem (at the panel level) should be solved, taking into account the information the pth panel receives, i.e., $\boldsymbol{\gamma}^{(i)}_{\text{agg},p-1}$, and its local SINR information $\boldsymbol{\gamma}_p$. After doing so, the aggregate SINR to be sent by panel p to panel $p+1$, at iteration i, is taken as,

$$\boldsymbol{\gamma}^{(i)}_{\text{agg},p} = \begin{cases} \underbrace{\boldsymbol{\gamma}^{(i)}_{\text{agg},p-1} - \tilde{\boldsymbol{\gamma}}^{(i-1)}_p}_{\text{A}} + \underbrace{\tilde{\boldsymbol{\gamma}}^{(i)}_p}_{\text{B}}, & p > 1 \\ \boldsymbol{\gamma}^{(i)}_{\text{agg},P} - \tilde{\boldsymbol{\gamma}}^{(i-1)}_p + \tilde{\boldsymbol{\gamma}}^{(i)}_p, & p = 1 \end{cases}, \tag{11}$$

[2]Depending on the panel selection and panel-terminal allocation, different max-min terminal rates can arise for the different iterations $i \in [1, I]$.

where:

- $\tilde{\boldsymbol{\gamma}}^{(i)}_p = [c^{(i)}_{p,(1)}\gamma_{p,(1)}, \ldots, c^{(i)}_{p,(K)}\gamma_{p,(K)}]$, with $\gamma_{p,(k)}$ being the SINR measured locally by each panel and given by (7), and $\boldsymbol{c}^{(i)}_p = [c^{(i)}_{p,(1)}, \ldots, c^{(i)}_{p,(K)}]$ the result of the terminal association to the pth panel at the ith iteration;
- If no terminal-panel is assumed a priori then $\boldsymbol{c}^{(0)}_p = \mathbf{0}_{1\times K}$, and as so, $\tilde{\boldsymbol{\gamma}}^{(0)}_p = \mathbf{0}_{1\times K}$.
- term A stands for the aggregated SINR at the pth panel at the ith iteration, but where panel p's contribution in iteration $i-1$ has been removed, thus being the aggregated SINR from all panels except the pth;
- term B is the contribution from panel p at iteration i to the aggregate SINR. This contribution will be (described in detail further below) returned by an optimisation that maximises the minimum SINR among all terminals at the ith iteration and when processing the pth panel.

Inspecting (11), it can be verified that the aggregate SINR for the pth panel can be expressed as,

$$\boldsymbol{\gamma}^{(i)}_{\text{agg},p} = \sum_{p'=p+1}^{P} \tilde{\boldsymbol{\gamma}}^{(i-1)}_{p'} + \sum_{p'=1}^{p} \tilde{\boldsymbol{\gamma}}^{(i)}_{p'}, \tag{12}$$

The local optimisation to be carried out at each panel to determine the term $\tilde{\boldsymbol{\gamma}}^{(i)}_p$ can be formulated as,

$$\tilde{\boldsymbol{\gamma}}^{(i)}_p = \left[c^{(i)}_{p,(1)}\gamma_{p,(1)}, \ldots, c^{(i)}_{p,(K)}\gamma_{p,(K)}\right] \text{ where}$$
$$c^{(i)}_{p,(k)} = \arg\max_{q_k} \quad \gamma_{\min},$$
subject to:
$$\gamma^{(i)}_{\text{agg},p,(k)} - c^{(i-1)}_{p,(k)}\gamma_{p,(k)} + q_k\gamma_{p,(k)} \geq \gamma_{\min}, \quad 1 \leq k \leq K,$$
$$\sum_{k=1}^{K} q_k = N,$$
$$q_k \in \{0, 1\}. \tag{13}$$

At iteration $i>1$, panel-terminal association is followed by panel selection. Panel p decides either to remain activate or to switch off, depending on its contribution for the max-min terminal rate delivered by panel P at iteration $i-1$. A panel remains active if and only if,

$$\frac{\min\left(\tilde{\boldsymbol{\gamma}}^{(i)}_p\right)}{\min\left(\boldsymbol{\gamma}^{(i-1)}_{\text{agg},P}\right)} \geq \beta, \tag{14}$$

where $\boldsymbol{\gamma}^{(i-1)}_{\text{agg},P}$ represents the aggregated SINR of panel P at the iteration $i-1$ and $\tilde{\boldsymbol{\gamma}}^{(i)}_p$ is the local SINR of panel p at iteration i after performing panel-terminal association. $\beta \in [0, 1]$ is used to measure the relevance of panel p. Particularly, the contribution of panel p at iteration i in relation to the max-min terminal rate at iteration $i-1$ must be higher or equal to β for panel p to remain active. The iterative process of panel selection and panel-terminal association is described in Algorithm 1.

Algorithm 1: Panel Selection and Panel-Terminal Association for a Sequential System Architecture.

Input: $\boldsymbol{\gamma}_p$, $\boldsymbol{c}_p^{(0)}$ (If no terminal-panel association is assumed a priori then $\boldsymbol{c}_p^{(0)} = \mathbf{0}_{1\times K}$), β, $\boldsymbol{\gamma}_{\text{agg},P}$

for $i = 1, \ldots, I$ **do**
  for $p = 1, \ldots, P$ **do**
    $[\tilde{\gamma}_p^{(i)}, \boldsymbol{c}_p^{(i)}] = \text{Solve (13)}$;
    if $i > 1$ **then**
      if $\min(\tilde{\boldsymbol{\gamma}}_p^{(i)}) < \min(\boldsymbol{\gamma}_{\text{agg},P}^{(i-1)})\beta$ **then**
        $\boldsymbol{c}_p^{(i)} = \mathbf{0}_{1\times K}$
        $\tilde{\boldsymbol{\gamma}}_p^{(i)} = \mathbf{0}_{1\times K}$
      end if
    end if
    $\boldsymbol{\gamma}_{\text{agg},p}^{(i)} = \boldsymbol{\gamma}_{\text{agg},p-1}^{(i)} - \tilde{\boldsymbol{\gamma}}_p^{(i-1)} + \tilde{\boldsymbol{\gamma}}_p^{(i)}$;
    Output at stage (i, p)**:** $\boldsymbol{c}_p^{(i)}$, $\boldsymbol{\gamma}_{\text{agg},p}^{(i)}$
  end for
end for

The max-min terminal rate at each (i, p) stage is thus given by,

$$R_{\min,p}^{(i)} = \mathbb{E}\left[\log_2\left(1 + \min(\boldsymbol{\gamma}_{\text{agg},p}^{(i)})\right)\right]. \tag{15}$$

As the number of communication rounds increases, the panel-terminal allocation in each panel becomes more reliable, thereby improving the max-min SINR among all terminals. At the beginning of the second iteration there is already a *big picture* of the panel-based LIS provided by $\boldsymbol{\gamma}_{\text{agg},P}^{(1)}$ at panel P, that is spread to the remaining panels along the 2nd iteration, enabling a faster convergence of (15) to (10).

B. FLOODING SYSTEM ARCHITECTURE

A flooding system architecture assumes P panels arranged in a grid as illustrated in Fig. 2. Each panel has direct connections with its neighbouring panels. For example, panel (r, s) (i.e., a centrally located panel) can connect to four neighbouring panels: $(r-1, s)$, $(r+1, s)$, $(r, s-1)$ and $(r, s+1)$. Panels positioned at the corners of the grid communicate with two or three neighbouring panels accordingly. As illustrated in Fig. 2, panel (r, s) receives, at iteration (i), average SINRs $\boldsymbol{\gamma}_{\text{avg},(r,s)}^{\uparrow,\text{in},(i)}$, $\boldsymbol{\gamma}_{\text{avg},(r,s)}^{\downarrow,\text{in},(i)}$, $\boldsymbol{\gamma}_{\text{avg},(r,s)}^{\rightarrow,\text{in},(i)}$, and $\boldsymbol{\gamma}_{\text{avg},(r,s)}^{\leftarrow,\text{in},(i)}$ from the neighbouring panels $(r+1, s)$, $(r-1, s)$, $(r, s-1)$ and $(r, s+1)$, respectively. For a panel (r, s) (i.e., a centrally located panel or located at a corner of the grid, the average received SINRs can be given by,

$$\boldsymbol{\gamma}_{\text{avg},(r,s)}^{\uparrow,\text{in},(i)} = \left[\gamma_{\text{avg},(r,s),(1)}^{\uparrow,\text{in},(i)}, \ldots, \gamma_{\text{avg},(r,s),(K)}^{\uparrow,\text{in},(i)}\right] = \begin{cases} \boldsymbol{\gamma}_{\text{avg},(r+1,s)}^{\uparrow,\text{out},(i-1)}, & r > 1 \\ 0, & \text{otherwise} \end{cases} \tag{16}$$

$$\boldsymbol{\gamma}_{\text{avg},(r,s)}^{\downarrow,\text{in},(i)} = \left[\gamma_{\text{avg},(r,s),(1)}^{\downarrow,\text{in},(i)}, \ldots, \gamma_{\text{avg},(r,s),(K)}^{\downarrow,\text{in},(i)}\right] = \begin{cases} \boldsymbol{\gamma}_{\text{avg},(r-1,s)}^{\downarrow,\text{out},(i-1)}, & r < R \\ 0, & \text{otherwise} \end{cases} \tag{17}$$

$$\boldsymbol{\gamma}_{\text{avg},(r,s)}^{\rightarrow,\text{in},(i)} = \left[\gamma_{\text{avg},(r,s),(1)}^{\rightarrow,\text{in},(i)}, \ldots, \gamma_{\text{avg},(r,s),(K)}^{\rightarrow,\text{in},(i)}\right] = \begin{cases} \boldsymbol{\gamma}_{\text{avg},(r,s-1)}^{\rightarrow,\text{out},(i-1)}, & s > 1 \\ 0, & \text{otherwise} \end{cases} \tag{18}$$

$$\boldsymbol{\gamma}_{\text{avg},(r,s)}^{\leftarrow,\text{in},(i)} = \left[\gamma_{\text{avg},(r,s),(1)}^{\leftarrow,\text{in},(i)}, \ldots, \gamma_{\text{avg},(r,s),(K)}^{\leftarrow,\text{in},(i)}\right] = \begin{cases} \boldsymbol{\gamma}_{\text{avg},(r,s+1)}^{\leftarrow,\text{out},(i-1)}, & s < S \\ 0, & \text{otherwise} \end{cases} \tag{19}$$

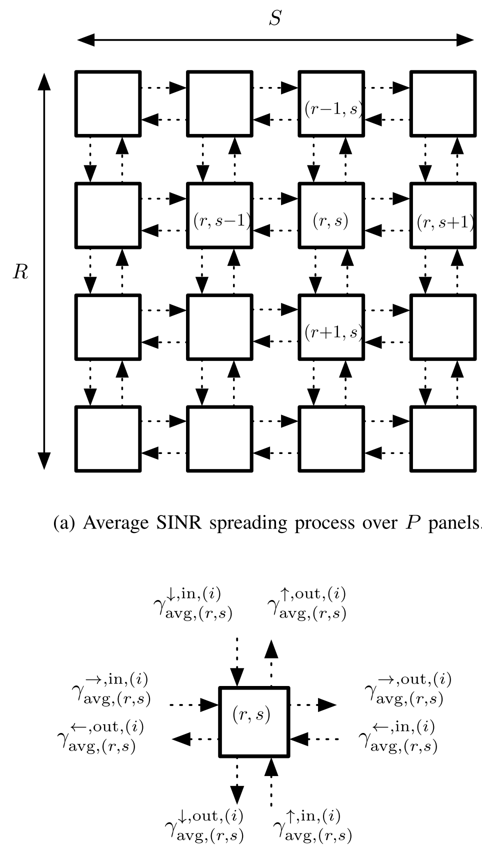

(a) Average SINR spreading process over P panels.

(b) The output/input SINR from/to panel (r, s).

FIGURE 2. Average SINR spreading process over $P = RS$ panels when considering a flooding scheme, for a given round of communication. In each round of communication, the P panels receive from each other and transmit to each other the average SINRs. One round of communication corresponds to a share of the average SINRs among all P panels.

where $\boldsymbol{\gamma}_{\text{avg},(r+1,s)}^{\uparrow,\text{out},(i-1)}$, $\boldsymbol{\gamma}_{\text{avg},(r-1,s)}^{\downarrow,\text{out},(i-1)}$, $\boldsymbol{\gamma}_{\text{avg},(r,s-1)}^{\rightarrow,\text{out},(i-1)}$, and $\boldsymbol{\gamma}_{\text{avg},(r,s+1)}^{\leftarrow,\text{out},(i-1)}$ are average SINRs calculated by panels $(r+1, s)$, $(r-1, s)$, $(r, s-1)$ and $(r, s+1)$ at iteration $(i-1)$ and transmitted by each corresponding neighbouring panel to panel (r, s); R denotes the number of panel positioned in a vertical manner; and S denotes the number of panel positioned in a horizontal manner. Table 1 presents a brief description of the variables

TABLE 1 Set of Average SINRs Exchanged Between Panel (r, s) and Its Neighbouring Panels

Variables	Description
$\gamma^{\uparrow,\text{in},(i)}_{\text{avg},(r,s)}$	set of average SINRs for the K terminals received by panel (r,s) and from panel $(r{+}1,s)$ at iteration i
$\gamma^{\downarrow,\text{in},(i)}_{\text{avg},(r,s)}$	set of average SINRs for the K terminals received by panel (r,s) and from panel $(r{-}1,s)$ at iteration i
$\gamma^{\rightarrow,\text{in},(i)}_{\text{avg},(r,s)}$	set of average SINRs for the K terminals received by panel (r,s) and from panel $(r,s{-}1)$ at iteration i
$\gamma^{\leftarrow,\text{in},(i)}_{\text{avg},(r,s)}$	set of average SINRs for the K terminals received by panel (r,s) and from panel $(r,s{+}1)$ at iteration i
$\gamma^{\uparrow,\text{out},(i)}_{\text{avg},(r,s)}$	set of average SINRs for the K terminals sent by panel (r,s) to panel $(r{-}1,s)$ at iteration i
$\gamma^{\downarrow,\text{out},(i)}_{\text{avg},(r,s)}$	set of average SINRs for the K terminals sent by panel (r,s) to panel $(r{+}1,s)$ at iteration i
$\gamma^{\rightarrow,\text{out},(i)}_{\text{avg},(r,s)}$	set of average SINRs for the K terminals sent by panel (r,s) to panel $(r,s{+}1)$ at iteration i
$\gamma^{\leftarrow,\text{out},(i)}_{\text{avg},(r,s)}$	set of average SINRs for the K terminals received by panel (r,s) to panel $(r,s{-}1)$ at iteration i

representing the set of average SINRs exchanged between the (r, s) panels and its neighbouring panels.

In a manner analogous to the sequential system architecture, the average SINRs $\boldsymbol{\gamma}^{\uparrow,\text{out},(i-1)}_{\text{avg},(r-1,s)}$, $\boldsymbol{\gamma}^{\downarrow,\text{out},(i-1)}_{\text{avg},(r+1,s)}$, $\boldsymbol{\gamma}^{\leftarrow,\text{out},(i-1)}_{\text{avg},(r,s-1)}$, and $\boldsymbol{\gamma}^{\rightarrow,\text{out},(i-1)}_{\text{avg},(r,s+1)}$ are then used to perform local terminal assignment, in which a panel only selects N from the set of K terminals to serve, aiming at maximising the minimum SINR among all K users. In particular, an average aggregated SINR $\boldsymbol{\gamma}^{(i)}_{\text{avg},(r,s)}$ calculated using the average SINRs $\boldsymbol{\gamma}^{\uparrow,\text{out},(i-1)}_{\text{avg},(r-1,s)}$, $\boldsymbol{\gamma}^{\downarrow,\text{out},(i-1)}_{\text{avg},(r+1,s)}$, $\boldsymbol{\gamma}^{\leftarrow,\text{out},(i-1)}_{\text{avg},(r,s-1)}$, and $\boldsymbol{\gamma}^{\rightarrow,\text{out},(i-1)}_{\text{avg},(r,s+1)}$ is used to perform local terminal assignment. The average aggregated SINR $\boldsymbol{\gamma}^{(i)}_{\text{avg},(r,s)}$, such as an aggregated SINR over i iterations, for panel (r, s) can be given by,

$$\boldsymbol{\gamma}^{(i)}_{\text{avg},(r,s)} = \frac{1}{i}\sum_{j=1}^{i} \gamma^{(j)}_{\text{agg},(r,s)} \tag{20}$$

with $\boldsymbol{\gamma}^{(j)}_{\text{agg},(r,s)}$ denoting an aggregated SINR for panel (r, s) accounting for all the contributions from the neighbouring panels $(r-1, s)$, $(r{+}1, s)$, $(r, s-1)$ and $(r, s{+}1)$ that can be given by,

$$\boldsymbol{\gamma}^{(i)}_{\text{agg},(r,s)} = \boldsymbol{\gamma}^{\uparrow,\text{in},(i)}_{\text{avg},(r,s)} + \boldsymbol{\gamma}^{\downarrow,\text{in},(i)}_{\text{avg},(r,s)} + \boldsymbol{\gamma}^{\rightarrow,\text{in},(i)}_{\text{avg},(r,s)} + \boldsymbol{\gamma}^{\leftarrow,\text{in},(i)}_{\text{avg},(r,s)} \tag{21}$$

In order for the panel (r, s) to choose which N terminals, an optimisation problem (at the panel level) should be solved, taking into account the average aggregated SINR and its local SINR information $\tilde{\boldsymbol{\gamma}}^{(i)}_{(r,s)}$. The local optimisation problem to be carried by each panel to determine the local SINR $\gamma_{(r,s),(k)}$ is based on the optimisation problem (9), in which the first constraint is replaced by $\sum_{p=1}^{P} c_{p,(k)}\gamma_{\text{avg},(r,s),(k)} \geq \gamma_{\min}$ and second replace by $\sum_{k=1}^{K} c_{p,(k)} = N$. The average SINR to be sent by panel (r, s) to neighbouring panels $(r, s{+}1)$, $(r, s-1)$, $(r{+}1, s)$ and $(r-1, s)$, at iteration i, is given by [3],

$$\boldsymbol{\gamma}^{\rightarrow,\text{out},(i)}_{\text{avg},(r,s)} = \boldsymbol{\gamma}^{\rightarrow,\text{in},(i)}_{\text{avg},(r,s)} + \boldsymbol{\gamma}^{\downarrow,\text{in},(i)}_{\text{avg},(r,s)} + \boldsymbol{\gamma}^{\uparrow,\text{in},(i)}_{\text{avg},(r,s)} + \tilde{\boldsymbol{\gamma}}^{(i)}_{(r,s)} \tag{22}$$

$$\boldsymbol{\gamma}^{\leftarrow,\text{out},(i)}_{\text{avg},(r,s)} = \boldsymbol{\gamma}^{\leftarrow,\text{in},(i)}_{\text{avg},(r,s)} + \boldsymbol{\gamma}^{\downarrow,\text{in},(i)}_{\text{avg},(r,s)} + \boldsymbol{\gamma}^{\uparrow,\text{in},(i)}_{\text{avg},(r,s)} + \tilde{\boldsymbol{\gamma}}^{(i)}_{(r,s)} \tag{23}$$

$$\boldsymbol{\gamma}^{\uparrow,\text{out},(i)}_{\text{avg},(r,s)} = \boldsymbol{\gamma}^{\uparrow,\text{in},(i)}_{\text{avg},(r,s)} + \tilde{\boldsymbol{\gamma}}^{(i)}_{(r,s)} \tag{24}$$

$$\boldsymbol{\gamma}^{\downarrow,\text{out},(i)}_{\text{avg},(r,s)} = \boldsymbol{\gamma}^{\downarrow,\text{in},(i)}_{\text{avg},(r,s)} + \tilde{\boldsymbol{\gamma}}^{(i)}_{(r,s)} \tag{25}$$

where:

- $\tilde{\boldsymbol{\gamma}}^{(i)}_{(r,s)} = [c^{(i)}_{(r,s),(1)}\gamma_{(r,s),(1)}, \ldots, c^{(i)}_{(r,s),(K)}\gamma_{(r,s),(K)}]$, with $\gamma_{(r,s),(k)}$ being the SINR measured locally by panel (r, s) and given by (7), and $\boldsymbol{c}^{(i)}_{(r,s)} = [c^{(i)}_{(r,s),(1)}, \ldots, c^{(i)}_{(r,s),(K)}]$ the result of the terminal association to the panel (r, s) at the ith iteration;
- If no terminal-panel is assumed a priori then $\boldsymbol{c}^{(0)}_{(r,s)} = \boldsymbol{0}_{1\times K}$, and as so, $\tilde{\boldsymbol{\gamma}}^{(0)}_{(r,s)} = \boldsymbol{0}_{1\times K}$;
- $\tilde{\boldsymbol{\gamma}}^{(i)}_{(r,s)}$ is the contribution from panel (r, s) at iteration i to the average SINR to be transmitted to the neighbouring panels. This contribution can be calculated by solving a local optimisation that maximises the minimum SINR among all terminals at the ith iteration and when processing the panel (r, s).

As illustrated by (22), (23), (24), and (25), panel (r, s) transmits different SINR information to each of the neighbouring panels $(r + 1, s)$, $(r - 1, s)$, $(r, s - 1)$, $(r, s + 1)$. Such message flowing technique is described in [8] and enables contributions of panel (r, s), such as the local SINR calculated at each panel based on the contributions received by neighbouring panels, to flow to the remaining panels by means of the neighbouring panels, with each panel using such local contribution only once. Note that the remaining panels are panels that do not have a direct connection with panel (r, s). In addition, the average SINRs received by panel (r, s) from the neighbouring panels $(r + 1, s)$, $(r - 1, s)$, $(r, s - 1)$, $(r, s + 1)$ may include average SINRs from previous iterations. However, the importance of previous iterations starts to decrease as the number of iterations increases. In other words, looking at a given SINR contribution for simplicity purposes, the SINR contribution is distributed across the panel-based LIS during each iteration, meaning that by the end of an iteration, the contribution has reached all panels. Such SINR contribution may still persist in a subsequent iteration, although with reduced relevance, which, as will be shown in Section VI, it does not prevent the flooding algorithm from converging to the max-min terminal rate of the centralized system architecture.

In a manner analogous to the sequential system architecture, at iteration $i{>}1$, panel-terminal association is followed by panel selection. Panel (r, s) decides whether to remain active or to turn off based on the average aggregated SINR

[3]Equations (22), (23), and (24), and (25) can be extended for any panel of the P panels and iteration. Consequently, equations (16), (17), (18), and (19) can be also linked to the previously mentioned equations, leading to equations 20 and 21 for any panel and iteration.

Algorithm 2: Panel Selection and Panel-Terminal Association for a Flooding System Architecture.

Input: $\boldsymbol{\gamma}_{\text{avg},(r,s)}$, $\boldsymbol{c}^{(0)}_{(r,s)}$ (If no terminal-panel association is assumed a priori then $\boldsymbol{c}^{(0)}_{(r,s)} = \mathbf{0}_{1\times K}$), β, $\tilde{\boldsymbol{\gamma}}^{(i)}_{\text{avg},(r,s)}$,
for $i = 1, \ldots, I$ **do**
  for $r = 1, \ldots, R$ **do**
    for $s = 1, \ldots, S$ **do**
      $[\tilde{\boldsymbol{\gamma}}^{(i)}_{\text{avg},(r,s)}, \boldsymbol{c}^{(i)}_{(r,s)}]$ = Solve (9) adapted to Flooding;
      if $\min(\tilde{\boldsymbol{\gamma}}^{(i)}_{\text{avg},(r,s)}) \neq 0 \wedge \min(\tilde{\boldsymbol{\gamma}}^{(i)}_{(r,s)}) < \min(\tilde{\boldsymbol{\gamma}}^{(i)}_{\text{avg},(r,s)})\beta$ **then**
        $\boldsymbol{c}^{(i)}_{(r,s)} = \mathbf{0}_{1\times K}$
        $\tilde{\boldsymbol{\gamma}}^{(i)}_{(r,s)} = \mathbf{0}_{1\times K}$
      end if
      Output at stage (i, r, s)**:** $\boldsymbol{c}^{(i)}_{(r,s)}$, $\tilde{\boldsymbol{\gamma}}^{(i)}_{(r,s)}$
    end for
  end for
end for

$\boldsymbol{\gamma}^{(i)}_{\text{avg},(r,s)}$ calculated at iteration i. If panel (r, s) chooses to remain active, based on the local terminal assignment, the average SINR $\boldsymbol{\gamma}^{(i)}_{\text{agg},p}$ at the panel is updated and passed to the neighbouring panels. In case panel (r, s) decides to switch off, it needs merely to pass the average SINR coming from the neighbouring panels to the same neighbouring panels at iteration $(i + 1)$. In a manner analogous to the sequential system architecture, no panels are switched off at iteration $i = 1$. Instead, only panel-terminal association is performed to establish an initial max-min terminal rate achieved at each panel. Panel selection together with panel-terminal association are then performed for iterations $i>1$. A panel remains active if and only if,

$$\min\left(\tilde{\boldsymbol{\gamma}}^{(i)}_{\text{avg},(r,s)}\right) = 0 \vee \frac{\min\left(\tilde{\boldsymbol{\gamma}}^{(i)}_{(r,s)}\right)}{\min\left(\tilde{\boldsymbol{\gamma}}^{(i)}_{\text{avg},(r,s)}\right)} \geq \beta, \tag{26}$$

where $\tilde{\boldsymbol{\gamma}}^{(i)}_{\text{avg},(r,s)}$ represents the average aggregated SINR of panel (r, s) at the iteration i and $\tilde{\boldsymbol{\gamma}}^{(i)}_{(r,s)}$ is the local SINR of panel (r, s) at iteration i after performing panel-terminal association. $\beta \in [0, 1]$ is used to measure the relevance of panel (r, s). In particular, the panel (r, s) must remain active when $\min(\tilde{\boldsymbol{\gamma}}^{(i)}_{\text{avg},(r,s)}) = 0$ as not all terminals are being served. In addition, the contribution of panel (r, s) at iteration i in relation to the average aggregated SINR calculated by panel (r, s) at iteration i based on SINR contributions of neighbouring panels must be higher or equal to β for the panel (r, s) to remain active. The iterative process of panel selection and panel-terminal association is described in Algorithm 2.

The max-min terminal rate at each (i, r, s) stage is thus given by,

$$r^{(i)}_{\min,(r,s)} = \mathbb{E}\left[\log_2\left(1 + \min\left(\boldsymbol{\gamma}^{\downarrow,\text{out},(i)}_{\text{avg},(r,s)}, \times \boldsymbol{\gamma}^{\uparrow,\text{out},(i)}_{\text{avg},(r,s)}, \boldsymbol{\gamma}^{\leftarrow,\text{out},(i)}_{\text{avg},(r,s)}, \boldsymbol{\gamma}^{\rightarrow,\text{out},(i)}_{\text{avg},(r,s)}\right)\right)\right]. \tag{27}$$

In a manner analogous to the sequential system architecture, the panel-terminal allocation in each panel becomes more reliable as the number of communication rounds increases, thereby improving the max-min SINR among all terminals. One round of communication corresponds to a communication stage when the RS panels have shared their SINR information with respective neighbouring panels. In other words, one round communication is a communication stage when all RS panels have received the SINR contributions from respective neighbouring panels and determined the average SINR to be sent to each of the respective neighbouring panels in the next round of communications, such as average SINRs $\boldsymbol{\gamma}^{\downarrow,\text{out},(i)}_{\text{avg},(r,s)}$, $\boldsymbol{\gamma}^{\uparrow,\text{out},(i)}_{\text{avg},(r,s)}$, $\boldsymbol{\gamma}^{\leftarrow,\text{out},(i)}_{\text{avg},(r,s)}$, and $\boldsymbol{\gamma}^{\rightarrow,\text{out},(i)}_{\text{avg},(r,s)}$.

VI. RESULTS AND DISCUSSION

In this section, the max-min terminal rate $R_{\min}$ for centralized, sequential and flooding system architectures is presented and compared. A LIS-panel based grid with $P \in \{25, 49\}$ panels is considered, each one with $M = 100$ antennas and $N \in \{2, \ldots, 6\}$ baseband outputs, serving $K \in \{10, 20, 30, 40\}$ terminals, which are uniformly distributed within the LIS area.

In all simulations, we assume unitary transmitted power per terminal, MF equalisation upon uplink detection, and a noise density of $N_0 = 10^{-4}$ (W/Hz). It is considered a transmission over a channel subject to multipath fading, pathloss and shadowing, with $\ell = 3.8$dB and $\sigma_{\text{shad}} = 8$dB [24], and perfect channel estimation at the LIS.

The centralized system approach uses the MILP solver provided by CPLEX to perform panel-terminal association and/or panel selection according to (9). For the sequential and and flooding system architecture, a solver is used to solve (13) and a properly adapted problem based on (9), respectively, that selects the K worst served terminals fulfilling the maximisation of the minimum rate among all terminals, using such information to activate or deactivate a panel when performing panel selection.'

A step shall be understood as a round of communication. In the context of the sequential system architecture, one iteration includes P rounds of communication, in which all P panels share the aggregate SINR (given by (11)) within the iteration. In the context of the flooding system architecture, one iteration includes $P = RS$ rounds of communication, in which all P panels share the average SINR (given by (22), (23), (24), and (25)) with its neighbouring panels within the iteration.

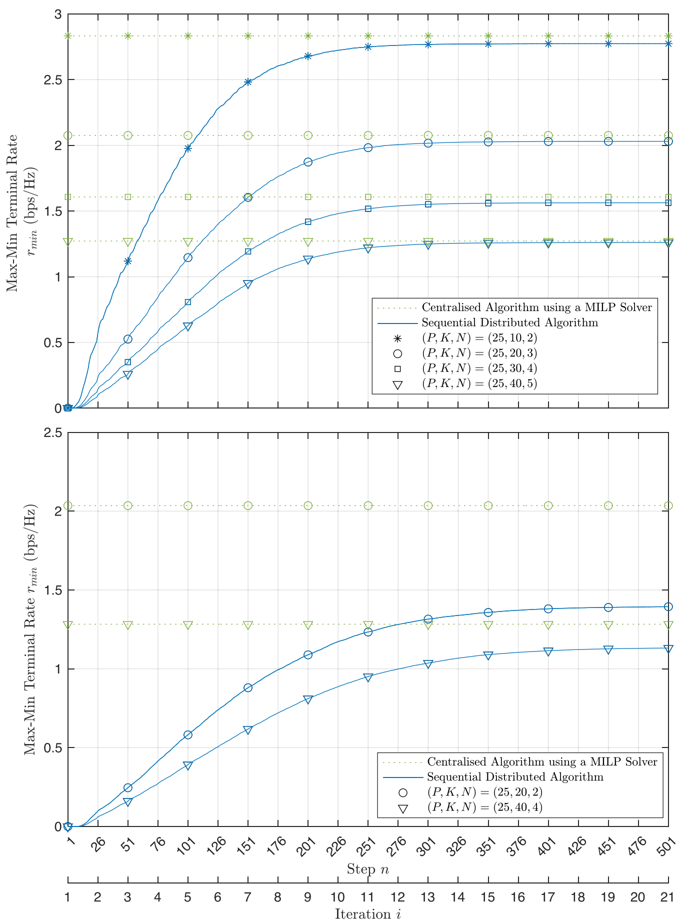

FIGURE 3. **Max-min terminal rate (bps/Hz) for centralized and sequential system architectures, when considering a panel-based LIS comprising $P = 25$ panels, for $K\in\{10, 20, 30, 40\}$ and number of baseband outputs $N\in\{2, 3, 4, 5\}$, when performing joint panel selection and panel-terminal association.**

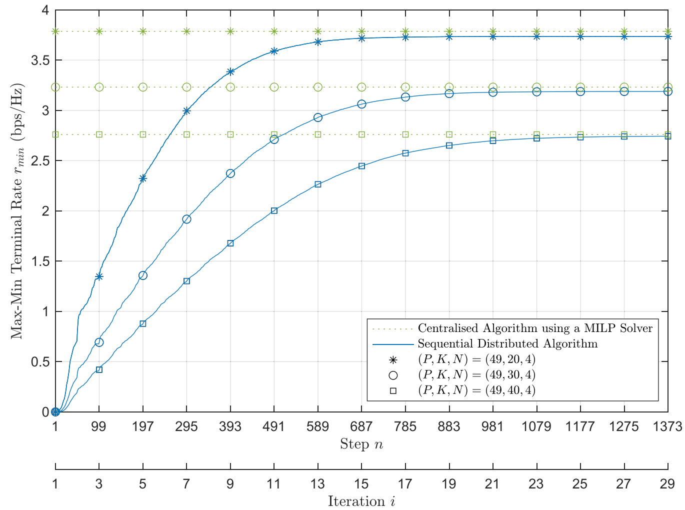

FIGURE 4. **Max-min terminal rate (bps/Hz) for centralized and sequential system architectures, when considering a panel-based LIS comprising $P = 49$ panels, for $K\in\{20, 30, 40\}$ and number of baseband outputs $N = 4$, when performing joint panel selection and panel-terminal association.**

A. CENTRALIZED VERSUS SEQUENTIAL DISTRIBUTED SYSTEM ARCHITECTURES

Figs. 3 and 4 illustrate the max-min terminal rate when $\beta = 0.2$ for both centralized and sequential distributed system architectures, when varying the LIS size (i.e, P). Each simulation in this subsection is performed generating 1000 channel realisations. Both Figs. 3 and 4 show a similar behaviour and the following observations are considered valid for both cases:

- It is observed that the max-min terminal rate achieved when employing the sequential distributed algorithm can fully converge to the one achieved when employing using the MILP solver.
- To ensure rate equality between both system architectures, a minimum number of baseband outputs per panel must be ensured, which can be observed by comparing curves of $(P, K, N) = (25, 20, 2)$ and $(P, K, N) = (25, 20, 3)$ or $(P, K, N) = (25, 40, 4)$ and $(P, K, N) = (25, 40, 5)$. In particular, the number of baseband outputs per panel must be at least $N\in\{2, 3, 4, 5\}$ for $P = 25$ and $K\in\{10, 20, 30, 40\}$, and $N = 4$ for $P = 49$ and for all $K\in\{20, 30, 40\}$, respectively;
- Sequential distributed system architectures yielding combinations of $(P, K, N) = (25, 10, 2); (25, 20, 3); (25, 30, 4); (25, 40, 5)$ require around 13 iterations for full rate convergence. On the other hand, sequential distributed system architectures yielding combinations of $(P, K, N) = (49, 20, 4); (49, 30, 4); (49, 40, 4)$ require around 17 to 21 iterations for full rate convergence. Hence, it is expected that a higher $K/(NP)$ ratio leads to a slower convergence (or no convergence at all), for a given number of panels P. For example, combination $(P, K, N) = (49, 20, 4)$ has a ratio $K/(NP)$ which is lower than combinations $(P, K, N) = (49, 30, 4); (49, 40, 4)$, thereby yielding a better ratio convergence. Combinations $(P, K, N) = (49, 40, 4); (25, 10, 2)$ provide approximately the same $K/(NP)$ ratio, thus offering similar max-min terminal rates and convergence rates. Furthermore, a slower convergence or no convergence can also be verified for the same configuration of P panels and K users yielding a lower number of baseband outputs per panel N. Such no convergence can be shown when comparing curves $(P, K, N) = (25, 20, 2); (25, 20, 3)$ or $(P, K, N) = (25, 40, 4); (25, 40, 5)$. In summary, an increase in the number of terminals K can lead to a lower rate convergence if, for a given number of panels P, the number of baseband outputs N is not increased accordingly.
- It is observed that the max-min SINR is zero (equivalent to have $r_{\min} = 0$) in the first steps, which means that not all terminals are being served. This is something expected from the sequential SINR sharing algorithm. In particular, at step 1 and iteration 1, panel 1 can only serve

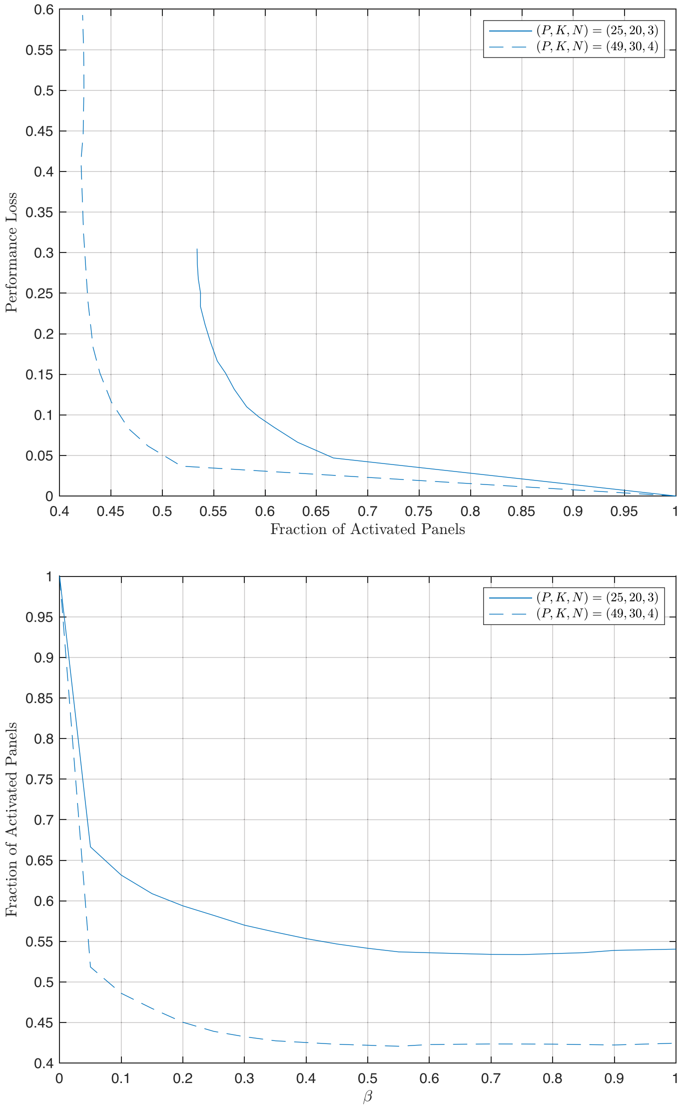

FIGURE 5. **Performance loss in the max-min terminal rate for the sequential panel selection and panel-terminal association algorithm, a given fraction of activated panels τ, a given $\beta\in[0,1]$, when considering a panel-based LIS comprising $P\in\{25,49\}$ panels, for $K\in\{20,30\}$, respectively, and number of baseband outputs $N\in\{3,4\}$.**

N users. Since $K>N$, it is expected to have the terminals waiting for being assigned to a given panel in the next steps at iteration 1 (i.e., the first round of communication). In the following iterations, it is guaranteed to have all terminals served.

B. PERFORMANCE LOSS FOR A SEQUENTIAL DISTRIBUTED SYSTEM ARCHITECTURE

Fig. 5 shows the performance loss in the max-min terminal rate when considering a sequential distributed system architecture (e.g., when employing a sequential panel selection and panel-terminal association algorithm), such performance loss being measured as the ratio between such rate with reference to the one achieved when employing a centralized system architecture, for a given fraction of activated panels τ, a given $\beta\in[0,1]$, combinations $(P,K,N)=(25,20,3)$; $(49,30,4)$. $(P,K,N)=(25,20,3)$; $(49,30,4)$ have been chosen simply because they allow convergence to the max-min rate of the centralized system architecture and a reasonable values of P, K, and N. When $\beta=0$, all P panels are activated and actively communicating with the K terminals. Simulations for combinations $(P,K,N)=(25,20,3)$; $(49,30,4)$ of Fig. 5 are performed generating 10000 and 4000 channel realisations, respectively.

Fig. 5 shows that lower values of β imply high-to-moderate fractions of activated panels and therefore lower performance losses. The maximum performance loss is of 30% for $(P,K,N)=(25,20,3)$ and 60% for $(P,K,N)=(49,30,4)$, meaning a minimum fraction of activated panels of 54% and 44%, respectively. Therefore, the worst case scenario for both combinations may already represent a decent choice. Furthermore, it is observed that such performance loss can be easily decreased by choosing a lower value of β, whose choice is dependent on the performance loss considered to be reasonable.

Fig. 6 shows the max-min terminal rate when $\beta=0.2$, for both centralized and sequential distributed system architectures. Simulations of Fig. 6 are performed generating 1000 channel realisations. It is shown that the saturation of both the max-min terminal rate and the fraction of activated panels for $(P,K,N)=(25,20,3)$ occurs at iteration $i=13$, whereas for $(P,K,N)=(49,30,4)$ it only occurs at iteration $i=19$. Nonetheless, it is reasonable to say that for the latter case, the fraction of activated panels remains approximately constant from iteration $i=9$, which can indicate that the saturation of both the max-min terminal rate and the fraction of activated panels does not necessarily happen at the same time. A possible explanation can be that, as the number of iterations increases, the deactivation of some panels leads to the activation of others and so on, until the max-min terminal rate saturates. An increase in the max-min terminal rate while verifying a constant fraction of activated panels may indicate that the activated panels at such time instant are not entirely the same while maintaining an equal quantity of panels. Therefore, it is valid to comment that,

- A higher number of panels requires more iterations (e.g., more communication rounds) to provide the best max-min terminal rate possible;
- A very small change in the number of activated panels can be decisive to deliver the best min-max terminal rate (especially when there is a higher number of panels).

Finally, it is noted that the difference in the fraction of activated panels in Figs. 5 and 6 can be explained by the number of channel realizations. For example, Figs. 5 and 6 show, for $\beta=0.2$, a fraction of activated panels of 45% and 60% for $(P,K,N)=(25,20,3)$ and of 59% and 75% for $(P,K,N)=(49,30,4)$. Simulations for the such combinations of Fig. 5 are performed generating 10000 and 4000 channel realisations, respectively, instead of 1000 channel realisations as for Fig. 6, showing that generating more channel realizations allows convergence to a global maximum.

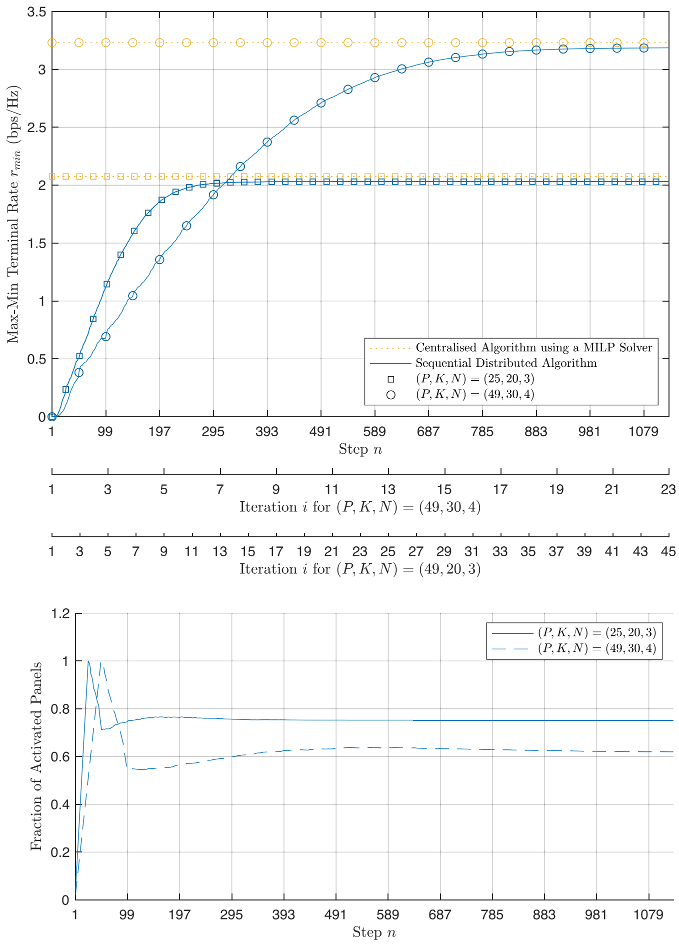

FIGURE 6. **Max-min terminal rate (bps/Hz) for centralized and sequential system architectures, when considering a panel-based LIS comprising $P\in\{25, 49\}$ panels, for $K\in\{20, 30\}$, respectively, and number of baseband outputs $N\in\{3, 4\}$, for $\beta = 0.2$.**

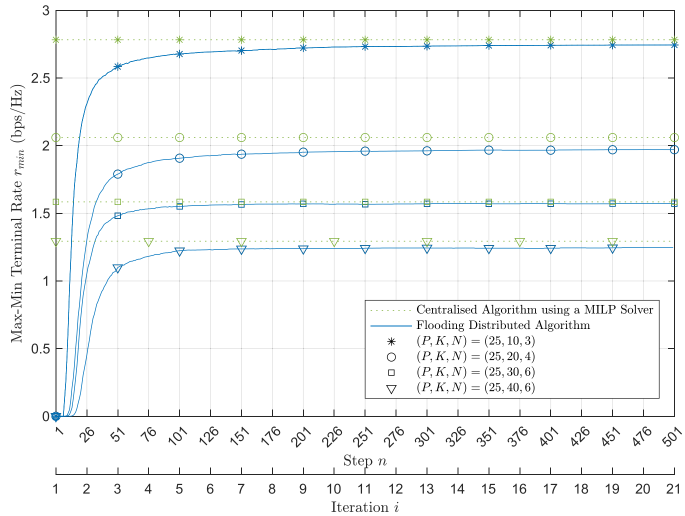

FIGURE 7. **Max-min terminal rate (bps/Hz) for centralized and flooding system architectures, when considering a panel-based LIS comprising $P = 25$ panels, for $K\in\{10, 20, 30, 40\}$ and number of baseband outputs $N\in\{3, 4, 6, 6\}$, when performing joint panel selection and panel-terminal association.**

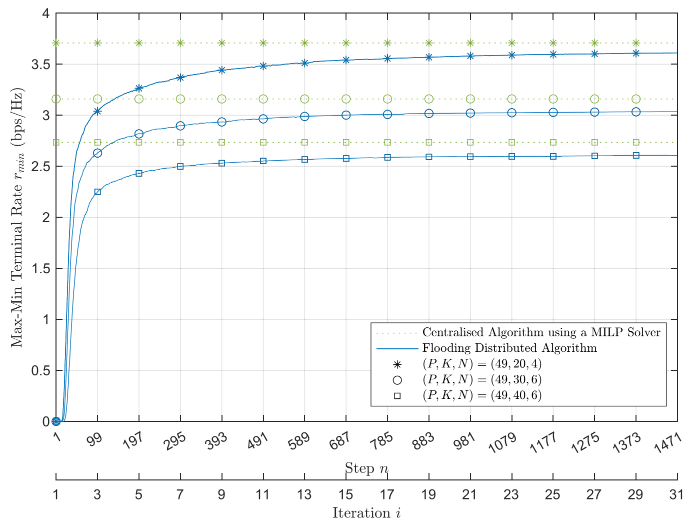

FIGURE 8. **Max-min terminal rate (bps/Hz) for centralized and flooding system architectures, when considering a panel-based LIS comprising $P = 49$ panels, for $K\in\{20, 30, 40\}$ and number of baseband outputs $N\in\{4, 6, 6\}$, when performing joint panel selection and panel-terminal association.**

C. CENTRALIZED VERSUS FLOODING DISTRIBUTED SYSTEM ARCHITECTURES

Figs. 7 and 8 illustrate the max-min terminal rate when $\beta = 0.2$ for both centralized and flooding system architectures, when varying the LIS size (i.e, P). Each simulation in this subsection is performed generating 1000 channel realisations.

Figs. 7 and 8 show a similar behaviour and the following observations are considered valid for both cases:

- It is observed that the max-min terminal rate achieved when employing the flooding distributed algorithm can (either almost or fully) converge to the one achieved when employing the MILP solver.
- Flooding distributed system architectures yielding combinations of $(P, K, N) = (25, 10, 3); (25, 20, 4); (25, 30, 6); (25, 40, 6)$ require around 5 to 9 iterations for full and/or almost rate convergence. On the other hand, flooding distributed system architectures yielding combinations of $(P, K, N) = (49, 20, 4); (49, 30, 6); (49, 40, 6)$ do not provide full rate convergence. However, the gap between the max-min terminal rate of a flooding distributed system architecture with the max-min terminal rate of a centralized system architecture is 0.14, which is a minor gap, showing that it is still viable to adopt a flooding distributed system architecture instead of a centralized system architecture.
- Saturation of the max-min SINR requires less iterations for higher $K/(NP)$ ratios. As illustrated by Fig. 7, saturation of the max-min SINR requires around 5 to 9 iterations, depending on the combination of (P, K, N). Fig. 8 shows that the max-min SINR requires around 13 to 21 iterations as combinations (P, K, N) of Fig. 8 yields a lower $K/(NP)$ ratio when compared to combinations (P, K, N) of Fig. 7.

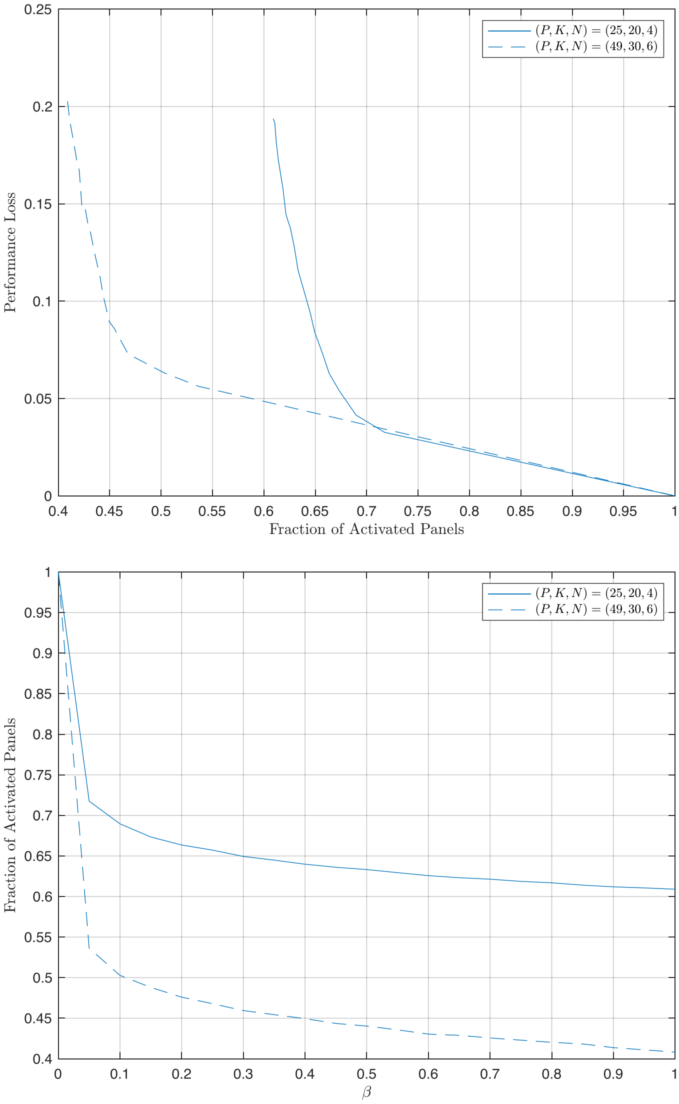

FIGURE 9. **Performance loss in the max-min terminal rate for the flooding panel selection and panel-terminal association algorithm, a given fraction of activated panels τ, a given $\beta\in[0, 1]$, when considering a panel-based LIS comprising $P\in\{25, 49\}$ panels, for $K\in\{20, 30\}$, respectively, and number of baseband outputs $N\in\{4, 6\}$.**

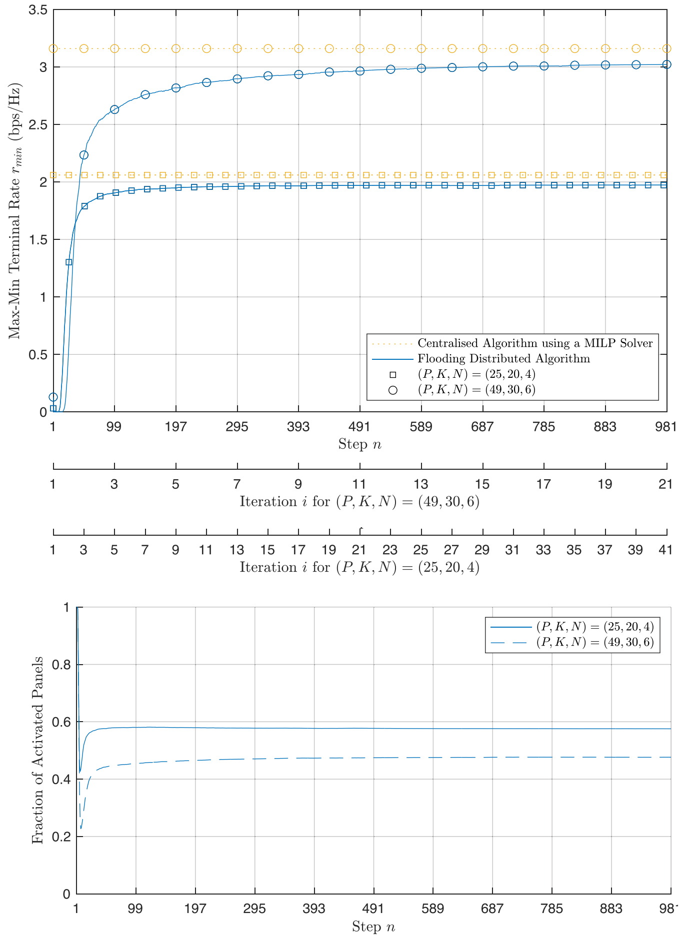

FIGURE 10. **Max-min terminal rate (bps/Hz) for centralized and flooding system architectures, when considering a panel-based LIS comprising $P\in\{25, 49\}$ panels, for $K\in\{20, 30\}$, respectively, and number of baseband outputs $N\in\{4, 6\}$, for $\beta = 0.2$.**

- In a manner analogous to the sequential system architecture, it is further verified that the max-min SINR is zero in the first steps of the first iteration. A panel flooding system architecture ensures that all the terminals can be served at the end of the first iteration, such as when the SINR information of each panel is received by all the remaining panels, either directly or via intermediate panels.

D. PERFORMANCE LOSS FOR A FLOODING DISTRIBUTED SYSTEM ARCHITECTURES

Fig. 9 shows the performance loss in the max-min terminal rate when considering a flooding distributed system architecture (e.g., when employing a flooding panel selection and panel-terminal association algorithm), such performance loss being measured as the ratio between such rate with reference to the one achieved when employing a centralized system architecture, for a given fraction of activated panels τ, a given $\beta\in[0, 1]$, combinations $(P, K, N) = (25, 20, 4); (49, 30, 6)$. When $\beta = 0$, all P panels are activated and actively communicating with the K terminals. Simulations for combinations $(P, K, N) = (25, 20, 4); (49, 30, 6)$ of Fig. 9 are performed generating 8000 and 4000 channel realisations, respectively.

In a manner analogous to the sequential system architecture, Fig. 9 shows that lower values of β can imply high-to-moderate fractions of activated panels and therefore lower performance losses. The maximum performance loss is of 19% for $(P, K, N) = (25, 20, 4)$ and 21% for $(P, K, N) = (49, 30, 6)$, meaning a minimum fraction of activated panels of 61% and 41%, respectively. Therefore, the worst case scenario for both combinations may already represent a decent choice. Furthermore, it is observed that such performance loss can be easily decreased by choosing a lower value of β, whose choice is dependent on the performance loss considered to be reasonable.

Fig. 10 shows the max-min terminal rate when $\beta = 0.2$, for both centralized and flooding distributed system architectures. Simulations of 10 are performed generating 1000 channel realisations. It should be noted that $(P, K, N) = (25, 20, 4)$; $(49, 30, 6)$ have been chosen simply because they allow convergence (or approximate convergence) to the max-min rate of the centralized system architecture and a reasonable values of P, K, and N. It is shown that the saturation of the max-min terminal rate for $(P, K, N) = (25, 20, 4)$ occurs at iteration $i = 9$, whereas for $(P, K, N) = (49, 30, 6)$ it only occurs at iteration $i = 13$. For example, for both combinations $(P, K, N) = (25, 20, 4)$ and $(P, K, N) = (49, 30, 6)$, saturation of the fraction of activated panels occurs before saturation of the max-min terminal rate. In particular, the fraction of activated panels remains approximately constant from iteration $i = 3$ for $(P, K, N) = (25, 20, 4)$ and from iteration $i = 8$ for $(P, K, N) = (49, 30, 4)$. Similar statements in Section VI-B can be used to explain these observations.

Finally, it is noted that the difference in the fraction of activated panels in Figs. 9 and 10 can be explained by the number of channel realizations, such as using the same rational as used in Section VI-B. Figs. 9 and 10 show, for the combination $(P, K, N) = (25, 20, 4)$, a similar fraction of activated panels (i.e., of 47%) for $\beta = 0.2$, showing that 1000 channel realisations allow convergence to a global maximum.

E. SEQUENTIAL VERSUS FLOODING DISTRIBUTED SYSTEM ARCHITECTURES

Regarding convergence speed to the max-min terminal rate achieved when employing a centralized system architecture, a flooding distributed system architecture (e.g., compare Fig. 3 with Fig. 7 or Fig. 4 with Fig. 8) can enable a faster convergence when compared to sequential distributed system architectures.

1) CONVERGENCE RATE TO THE CENTRALIZED MAX-MIX RATE

The sequential distributed system architecture can ensure fully or almost convergence to the max-min terminal rate achieved by a centralized system architecture (e.g., see Figs. 3 and 4). For the flooding distributed system architecture, as observed in Figs. 7 and 8, the gap between the max-min terminal rate achieved when employing the flooding distributed system architecture and the max-min terminal rate achieved when employing a centralized system architecture can be seen as minor, thereby showing that a flooding distributed system architecture can still be a viable choice for scenarios where approximate or fully convergence is required.

2) PERFORMANCE LOSS

A flooding distributed system architecture, compared to a sequential distributed system architecture, can achieve lower performance loss while ensuring a lower fraction of activated panels. Note that both the gap between the curves associated with the combinations $(P, K, N) = (25, 20, 3)$ and $(P, K, N) = (49, 30, 4)$ of Fig. 5 as well as the gap between the curves associated with the combinations $(P, K, N) = (25, 20, 4)$ and $(P, K, N) = (49, 30, 6)$ of Fig. 9 can be explained by the rate K/NP. In other words, a flooding distributed system architecture yields, when compared with the sequential system architecture, a larger gap since the difference between the rate K/NP associated with the combinations $(P, K, N) = (25, 20, 4)$ and $(P, K, N) = (49, 30, 6)$ is slightly greater than the difference between the rate K/NP associated with the combinations $(P, K, N) = (25, 20, 3)$ and $(P, K, N) = (49, 30, 3)$.

3) FINAL REMARKS

For both the sequential and flooding distributed system architectures, it is observed that, in order to ensure full or approximate convergence to the max-min terminal rate achieved by a centralized distributed system, specific combinations of (P, K, N) are required. It can also be noticed that, for both the sequential and flooding distributed system architectures, the rate K/NP associated with combinations of (P, K, N) providing such convergence increases when increasing the number of terminals K. Therefore, an increase in the number of baseband outputs per panel N may be required to ensure delivery of a proper max-min terminal rate (i.e., a terminal rate ensuring a good performance for the worst-served user) in a scenario where an increase in the number of terminals K is verified for a given number of panels P.

In general, a flooding distributed system architecture, when compared to the sequential distributed system architecture, requires a slightly higher number of baseband outputs N for the same number of panels P and number of terminals K for ensuring a decent convergence to the max-min terminal rate achieved by a centralized distributed system. On the other hand, saturation of the max-min terminal rate for a flooding distributed system architecture is verified for a lower number of iterations, thereby indicating that the SINR information is transmitted in a faster manner for a flooding distributed system architecture in comparison with a sequential distributed system architecture.

VII. CONCLUSION

In this paper, we propose panel selection and panel-terminal association algorithms for decentralized panel-based LIS communication systems. Such algorithms aim at allocating a set of terminals to a given panel, comprising a limited number of baseband outputs, while maximising the minimum terminal terminal rate. In particular, a sequential as well as a flooding process for spreading an aggregated SINR over all panels is considered.

In this paper, specific combinations of several system parameters (number of panels, number of terminals, number of baseband outputs per panels) required to ensure, for fully decentralized LIS-based system architectures, full or approximate convergence to a rate achieved by a centralized panel-based LIS have been provided. The fully decentralized LIS-based system architectures comprise a sequential system architecture and a flooding system architecture. The following observations should be taken into consideration when designing and configuring fully decentralized LIS-based communication systems for practical scenarios:

- For both fully decentralized LIS-based system architectures, a higher number of panels requires more iterations (e.g., more communication rounds between panels) to provide the rate ensuring fairness between terminals (i.e., min-max terminal rate). A very small change in the number of activated panels can be decisive to deliver the best min-max terminal rate (especially when there is a higher number of panels).
- For both fully decentralized LIS-based system architectures, an increase in the number of baseband outputs per panel may be required to ensure delivery of a proper max-min terminal rate in a scenario where an increase in the number of terminals is verified for a given number of panels.
- Both sequential and flooding system architectures offer decent convergence rates for the centralized max-min terminal rate when selecting proper combinations of the several system parameters, in turn ensuring scalability.
- Nonetheless, a flooding distributed system architecture, when compared to a sequential system architecture, requires a slightly higher number of baseband outputs for the same number of panels and number of terminals for ensuring such a decent convergence. On the other hand, saturation of the max-min terminal rate for a flooding system architecture is verified for a lower number of iterations, thereby indicating that the SINR information is transmitted in a faster manner. Hence, a flooding system architecture provides for decent convergences at the price of a slight increase in the number of baseband outputs per panel.

REFERENCES

[1] H. Tataria, F. Tufvesson, and O. Edfors, "Real-time implementation aspects of large intelligent surfaces," in *Proc. 2020 IEEE Int. Conf. Acoust., Speech Signal Process.*, 2020, pp. 9170–9174.

[2] A. Pereira, F. Rusek, M. Gomes, and R. Dinis, "On the complexity requirements of a panel-based large intelligent surface," in *Proc. 2020 IEEE Glob. Commun. Conf.*, 2020, pp. 1–6.

[3] A. Pereira, F. Rusek, M. Gomes, and R. Dinis, "The impact of terminal mobility on the performance of a panel-based large intelligent surface," in *Proc. 54th Asilomar Conf. Signals, Syst., Comput.*, 2020, pp. 569–573.

[4] J. R. Sánchez, F. Rusek, O. Edfors, M. Sarajlić, and L. Liu, "Decentralized massive MIMO processing exploring daisy-chain architecture and recursive algorithms," *IEEE Trans. Signal Process.*, vol. 68, pp. 687–700, 2020.

[5] C. Jeon, K. Li, J. R. Cavallaro, and C. Studer, "Decentralized equalization with feedforward architectures for massive MU-MIMO," *IEEE Trans. Signal Process.*, vol. 67, no. 17, pp. 4418–4432, Sep. 2019.

[6] K. Li, R. R. Sharan, Y. Chen, T. Goldstein, J. R. Cavallaro, and C. Studer, "Decentralized baseband processing for massive MU-MIMO systems," *IEEE Trans. Emerg. Sel. Topics Circuits Syst.*, vol. 7, no. 4, pp. 491–507, Dec. 2017.

[7] M. Sadeghi, C. Yuen, and Y. H. Chew, "Sum rate maximization for uplink distributed massive MIMO systems with limited backhaul capacity," in *Proc. 2014 IEEE Globecom Workshops*, 2014, pp. 308–313.

[8] J. V. Alegría, J. Rodríguez, F. Sánchez, L. R. Liu, and O. Edfors, "Decentralized equalizer construction for large intelligent surfaces," in *Proc. IEEE 90th Veh. Technol. Conf.*, 2019, pp. 1–6.

[9] J. R. Sánchez, O. Edfors, F. Rusek, and L. Liu, "Processing distribution and architecture tradeoff for large intelligent surface implementation," in *Proc. 2020 IEEE Int. Conf. Commun. Workshops*, 2020, pp. 1–6.

[10] J. V. Alegría, F. Rusek, J. R. Sánchez, and O. Edfors, "Modular binary tree architecture for distributed large intelligent surface," in *Proc. 2021 IEEE Int. Conf. Acoust., Speech Signal Process.*, 2021, pp. 4565–4569.

[11] J. R. Sánchez, F. Rusek, O. Edfors, and L. Liu, "Distributed and scalable uplink processing for LIS: Algorithm, architecture, and design tradeoffs," *IEEE Trans. Signal Process.*, vol. 70, pp. 2639–2653, 2022.

[12] J. Zhang, S. Chen, Y. Lin, J. Zheng, B. Ai, and L. Hanzo, "Cell-free massive MIMO: A new next-generation paradigm," *IEEE Access*, vol. 7, pp. 99878–99888, 2019.

[13] H. Q. Ngo, A. Ashikhmin, H. Yang, E. G. Larsson, and T. L. Marzetta, "Cell-free massive MIMO versus small cells," *IEEE Trans. Wireless Commun.*, vol. 16, no. 3, pp. 1834–1850, Mar. 2017.

[14] H. Q. Ngo, G. Interdonato, E. G. Larsson, G. Caire, and J. G. Andrews, "Ultradense cell-free massive MIMO for 6G: Technical overview and open questions," *Proc. IEEE*, vol. 112, no. 7, pp. 805–831, Jul. 2024.

[15] M. Bashar, K. Cumanan, A. G. Burr, M. Debbah, and H. Q. Ngo, "On the uplink max–min SINR of cell-free massive MIMO systems," *IEEE Trans. Wireless Commun.*, vol. 18, no. 4, pp. 2021–2036, Apr. 2019.

[16] E. Shi et al., "RIS-Aided cell-free massive MIMO systems for 6G: Fundamentals, system design, and applications," *Proc. IEEE*, vol. 112, no. 4, pp. 331–364, Apr. 2024.

[17] E. Björnson and L. Sanguinetti, "Making cell-free massive MIMO competitive with MMSE processing and centralized implementation," *IEEE Trans. Wireless Commun.*, vol. 19, no. 1, pp. 77–90, Jan. 2020.

[18] Z. H. Shaik, E. Björnson, and E. G. Larsson, "Cell-free massive MIMO with radio stripes and sequential uplink processing," in *Proc. 2020 IEEE Int. Conf. Commun. Workshops*, 2020, pp. 1–6.

[19] F. Conceição, M. Gomes, V. Silva, R. Dinis, and C. H. Antunes, "Joint spectral and power efficiency optimization in uplink radio stripes," *IEEE Trans. Commun.*, vol. 72, no. 8, pp. 5209–5225, Aug. 2024.

[20] F. Conceição, M. Gomes, V. Silva, and R. Dinis, "Streamlined swift allocation strategies for sequential fronthaul cell-free massive MIMO," *IEEE Access*, vol. 13, pp. 197562–197579, Nov. 2025.

[21] F. Conceição, C. H. Antunes, M. Gomes, V. Silva, and R. Dinis, "User fairness in radio stripes networks using meta-heuristics optimization," in *Proc. IEEE 95th Veh. Technol. Conf.: (VTC2022-Spring)*, 2022, pp. 1–6.

[22] G. Interdonato, E. Björnson, H. Q. Ngo, P. Frenger, and E. G. Larsson, "Ubiquitous cell-free massive MIMO communications," *EURASIP J. Wireless Commun. Netw.*, vol. 2019, no. 197, pp. 1–13, 2019.

[23] A. Pereira, F. Rusek, M. Gomes, and R. Dinis, "A low complexity sequential resource allocation for panel-based LIS surfaces," in *Proc. IEEE 95th Veh. Technol. Conference: (VTC2022-Spring)*, 2022, pp. 1–6.

[24] T. L. Marzetta, "Noncooperative cellular wireless with unlimited numbers of base station antennas," *IEEE Trans. Wireless Commun.*, vol. 9, no. 11, pp. 3590–3600, Nov. 2010.

ANDREIA PEREIRA was born in Coimbra, Portugal, in 1993. She is currently working toward the Ph.D. degree in electrical and computer engineering with the Faculty of Sciences and Technology, University of Coimbra, Coimbra, Portugal, with a mixed Ph.D. Grant supported by Fundação para a Ciência e a Tecnologia in partnership with the Department of Electrical and Information Theory, Lund University, Lund, Sweden. She has been a Student Researcher with the Instituto de Telecomunicações, where she is currently involved in wireless digital communications, massive-MIMO systems, large intelligent surfaces, frequency equalisation techniques, spatial resource allocation and general signal processing for communications.

FILIPE CONCEIÇÃO (Graduate Student Member, IEEE) was born in Coimbra, Portugal, in 1996. He received the M.Sc. degree in electrical and computer engineering speciality in telecommunications from the University of Coimbra, Coimbra, Portugal, in 2019, and the Ph.D. degree from the Department of Electrical and Computer Engineering, Faculty of Science and Technology, University of Coimbra and Instituto de Telecomunicações, in 2025. His research focus is on the development of transmission, detection, and resource allocation techniques for radio stripe systems. His current research interests include cooperative communications 6 G networks, including distributed massive MIMO, cell-free, radio stripe, resource allocation, and pre-coding/equalization techniques.

FREDRIK RUSEK was born in Lund, Sweden, in 1978. He received the M.S. and Ph.D. degrees in electrical engineering from Lund University, Lund, in 2003 and 2007, respectively. Since 2012, he has been an Associate Professor with the Department of Electrical and Information Technology, Lund Institute of Technology, Lund. His research interests include modulation theory, equalization, wireless communications, and applied information theory.

RUI DINIS (Senior Member, IEEE) received the Ph.D. degree from Instituto Superior Técnico (IST), Technical University of Lisbon, Lisbon, Portugal, in 2001, and the Habilitation in telecommunications from Faculdade de Ciências e Tecnologia (FCT), Universidade Nova de Lisboa (UNL), Lisbon, in 2010. From 2001 to 2008, he was a Professor with IST. In 2003, he was an invited Professor with Carleton University, Ottawa, ON, Canada. He was a Researcher with Centro de Análise e Processamento de Sinal, IST, from 1992 to 2005, and a Researcher with Instituto de Sistemas e Robótica from 2005 to 2008. Since 2009, he has been a Researcher with Instituto de Telecomunicações. He is currently an Associate Professor with FCT-UNL. He has been actively involved in several national and international research projects in the broadband wireless communications area. His research interests include transmission, estimation, and detection techniques. Rui Dinis is a VTS Distinguished Lecturer and is or was an Editor of IEEE TRANSACTIONS ON WIRELESS COMMUNICATIONS, IEEE TRANSACTIONS ON COMMUNICATIONS, IEEE TRANSACTIONS ON VEHICULAR TECHNOLOGY, IEEE OPEN JOURNAL ON COMMUNICATIONS, and Elsevier *Physical Communication*. He was also a Guest Editor for several special issues.

MARCO GOMES (Senior Member, IEEE) was born in Coimbra, Portugal, in 1977. He received the M.Sc. and Ph.D. degrees in electrical and computer engineering specialty in telecommunications in 2004 and 2011, respectively, from the University of Coimbra, Coimbra, Portugal, where he is currently an Assistant Professor with the Department of Electrical and Computer Engineering, Faculty of Science and Technology. He is also a Senior Researcher with Instituto de Telecomunicações and performs different collaborations under his research and development activities with other institutions and universities worldwide. His main research interests include wireless digital communications, massive-MIMO, large intelligent surfaces, general signal processing for communications, software-defined radio, error control coding, and physical layer security. He is a member of the IEEE Communications Society and the IEEE Vehicular Technology Society. Dr. Gomes is an Editor of the IEEE COMMUNICATIONS LETTERS, IEEE OPEN JOURNAL OF THE COMMUNICATIONS SOCIETY, IEEE ComSoc On-Line Content, and *Physical Communication* (Elsevier).